

Presented at: International Conf. on Dislocation Modeling in Physical Systems

MASTER

ON THE SIMULTANEOUS FORMATION OF INTERSTITIAL - AND VACANCY-TYPE LOOPS DURING IRRADIATION

A. Si-Ahmed and W.G. Wolfer

Fusion Engineering Program, Nuclear Engineering Department
University of Wisconsin, Madison, WI 53706, U.S.A.

Abstract

During the irradiation of metals at temperatures above Stage III, dislocation loops are formed. Both interstitial - and vacancy-type loops are observed. Their simultaneous formation is possible because of a difference in their capture efficiency for interstitials which is due to non-linear elasticity effects on the strain fields of loops. This difference is only a necessary condition for the nucleation of vacancy-type loops. Other conditions, such as temperature, dose rate, and the average interstitial capture efficiency of the entire sink structure, must also be met. These conditions are investigated, and it is found that vacancy loops can nucleate at low temperatures and when the capture efficiency of the entire sink structure exceeds a critical value. With continuing irradiation, both interstitial - and vacancy loops grow to large radii, and the capture efficiency drops below the critical value. At this point, further vacancy-loop nucleation is terminated.

Introduction

Radiation-induced changes of the dislocation structure in metals at temperatures above Stage III are driven by the preferential absorption of interstitials at edge dislocations. This preferential capture is the result of a drift diffusion of the point defects in the stress field of dislocations. According to previous calculations (1) the drift-induced currents of point defects to both interstitial - and vacancy-type loops are identical. It has, therefore, been always assumed that vacancy-type loops could not nucleate and grow simultaneously with interstitial-type loops. Nevertheless, there are numerous observations [references cited in (3)] attesting to the simultaneous growth of both types of loops.

To explain the apparent contradiction between the earlier theoretical predictions and these observations, two proposals have been advanced recently (2,3). Our explanation (2), to be discussed further in section 2, is based on the nonlinear elasticity contribution to the strain field of small dislocation loops. In contrast, Bullough, et al. (3) suggest that the proximity of other sinks affects the capture of the two loop types for interstitials to a different degree. The proximity effect is modelled by surrounding the loop by a cell boundary, and the cell volume is inversely proportional to the sink density. The difference in the capture efficiency of the two loop types is, therefore, substantial only for high densities.

In contrast, the capture efficiencies and the difference arising from nonlinear elasticity are intrinsic properties of the loops in our analysis. Proximity effects are negligible and unnecessary to explain the simultaneous formation of both types of loops.

A difference in preferential absorption at both loop types is only a necessary, but not a sufficient condition for vacancy-type loop formation. Other conditions must be met also for vacancy-type loops to nucleate. It is the purpose of this paper to investigate these other conditions. They arise from the fact that a significant nucleation barrier exists for vacancy-type loops, whereas practically none exists for interstitial-type loops (4).

Capture Efficiency of Dislocation Loops

The current of point defects to a circular dislocation loop of radius R can be written as

$$J = Z(R) [4\pi^2 R / \ln(8R/a)] D(C - C^2(R)) \quad (1)$$

where $Z(R)$ is the capture efficiency, which accounts for the drift of the point defects in the strain field of the dislocation. The remaining factors in Eq. (1) represent the point-defect

DISCLAIMER

This book was prepared as an account of work sponsored by an agency of the United States Government. Neither the United States Government nor any agency thereof, nor any of their employees, makes any warranty, express or implied, or assumes any legal liability or responsibility for the accuracy, completeness, or usefulness of any information, apparatus, product, or process disclosed, or represents that its use would not infringe privately owned rights. Reference herein to any specific commercial product, process, or service by trade name, trademark, manufacturer, or otherwise, does not necessarily constitute or imply its endorsement, recommendation, or favoring by the United States Government or any agency thereof. The views and opinions of authors expressed herein do not necessarily state or reflect those of the United States Government or any agency thereof.

DISTRIBUTION OF THIS DOCUMENT IS UNLIMITED

Rey

DISCLAIMER

This report was prepared as an account of work sponsored by an agency of the United States Government. Neither the United States Government nor any agency Thereof, nor any of their employees, makes any warranty, express or implied, or assumes any legal liability or responsibility for the accuracy, completeness, or usefulness of any information, apparatus, product, or process disclosed, or represents that its use would not infringe privately owned rights. Reference herein to any specific commercial product, process, or service by trade name, trademark, manufacturer, or otherwise does not necessarily constitute or imply its endorsement, recommendation, or favoring by the United States Government or any agency thereof. The views and opinions of authors expressed herein do not necessarily state or reflect those of the United States Government or any agency thereof.

DISCLAIMER

Portions of this document may be illegible in electronic image products. Images are produced from the best available original document.

current in the absence of the drift as given by Seeger and Goesele (5). Here, a is the dislocation pipe radius, D the diffusion coefficient, C the average point defect concentration, and

$$C^{\ell}(R) = C^{\text{eq}} \exp\{\Delta W(R)/kT\} \quad (2)$$

is the point defect concentration in local thermodynamic equilibrium with the dislocation loop. C^{eq} is the corresponding concentration in the ideal crystal, and $\Delta W(R)$ is the change in the energy of the loop when one point defect is absorbed.

The capture efficiency can be represented (2) by

$$Z(R) = \ln(8R/a) / \ln(8R/c) \quad (3)$$

where the capture radius c is greater than the pipe radius a . Both radii were determined by matching the expression (3) to results of the infinitesimal loop (1) for small R and to the results for the straight edge dislocation (6). Two sets of values, $a_i = 8 b_0$, $c_i = 20 b_0$, and $a_v = 2.7 b_0$, $c_v = 3.5 b_0$, are thereby obtained for the capture efficiencies Z_i and Z_v for interstitials and vacancies, respectively. All these radii are proportional to the Burgers vector b_0 . The latter is a measure of the magnitude of the strain field of the dislocation loop in the linear elasticity theory.

As shown recently (2), nonlinear elastic effects can be accounted for if b_0 is replaced by an apparent Burgers vector $b(R)$. Its value can be determined from the volume change δV_{ℓ} produced by the creation of dislocation loops. The volume of point defects contained in a loop is given by

$$V_{\ell} = \pm \pi R^2 b_0 + \delta V_{\ell} = \pm \pi R^2 b(R), \quad (4)$$

where the plus (minus) sign holds for an interstitial-type (vacancy-type) loop. The volume change δV_{ℓ} can be computed according to the Zener expression as given by Seeger and Haasen (8), if the pressure derivatives of the elastic constants are known. Using the derivatives for nickel from the recent compilation of Guinan and Steinberg (8), the apparent Burgers vector can be computed from Eq. (4). The results are shown in Figure 1. The ratio $b(R)/b_0$ is also equal to the ratio V_{ℓ}/V_{ℓ}^0 , where $V_{\ell}^0 = \pm \pi R^2 b_0$ is the volume of atoms inserted or extracted when creating the dislocation loop. In other words, V_{ℓ}/V_{ℓ}^0 is the volume per point defect contained in the loop divided by the atomic volume Ω . As seen from Fig. 1, the volume per point defect deviates from the atomic volume as the loop radius decreases. When extrapolated to one point defect, it is found that the volume relaxation due to an interstitial is equal to 1.81Ω , and the volume relaxation due to a vacancy is -0.18Ω . Both values are in good agreement with measured values of the relaxation volumes for interstitials and vacancies (9).

The apparent Burgers vector $b(R)$ can now be substituted for b_0 in the capture radii c_i and c_v to reflect the second-order elasticity effects on the loop strain field and on the capture efficiency ratio $Z_i(R)/Z_v(R)$. Since $b(R) > b_0$ for interstitial-type loops and $b(R) < b_0$ for vacancy-type loops, the two loops acquire different capture efficiencies. This difference decreases with increasing loop radius, as shown in Figure 2.

Vacancy Loop Nucleation

The formulation of a nucleation theory for vacancy-type loops is identical to the void nucleation theory as developed by Katz, Wiedersich (10) and Russell (11), except for the substitution of the point defect fluxes as given now by Eq. (1). Based on our previous formulation for void nucleation (12), the nucleation barrier $\Delta G(R)$ for vacancy-type loops depends on two important contributions. $\Delta G(R)$ increases as the net bias

$$Z_i(R)/Z_v(R) - \langle Z_i/Z_v \rangle$$

increases. Here, the capture efficiency ratio $\langle Z_i/Z_v \rangle$ is averaged over all the sinks in a manner defined previously (12). The second contribution to $\Delta G(R)$ arises from the difference in the thermal vacancy concentration

$$C_v^{\ell}(R) - \langle C_v \rangle$$

where $\langle C_v \rangle$ is the average vacancy concentration in thermal equilibrium with the sinks. Again, this average was defined previously (12).

In order to obtain the average vacancy and interstitial concentrations C_i and C_v the usual rate equations are solved for a given Frenkel pair production rate and a given recombination volume. The latter was computed with a recently derived expression (13) which shows excellent agreement at low temperature with measured values by Nakagawa et al. (14). At

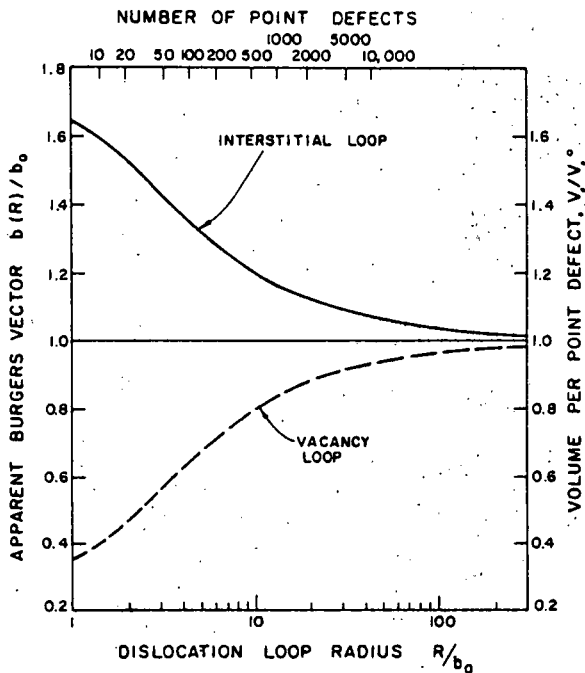


Figure 1 Apparent Burgers vector or relaxation volume per point defects contained in loops of given radius R . b_0 is the Burgers vector for the undeformed crystal.

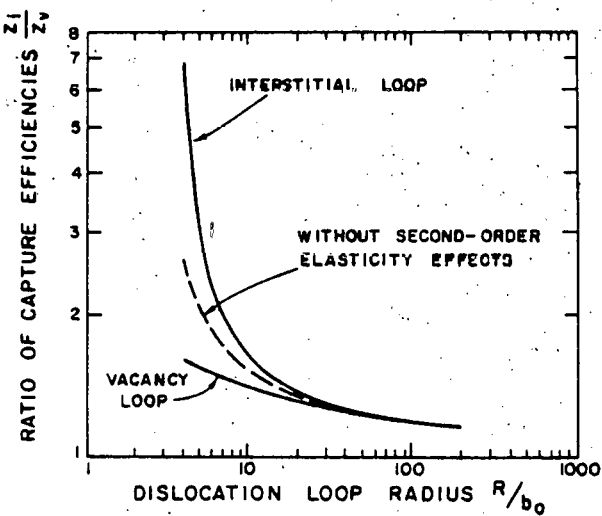
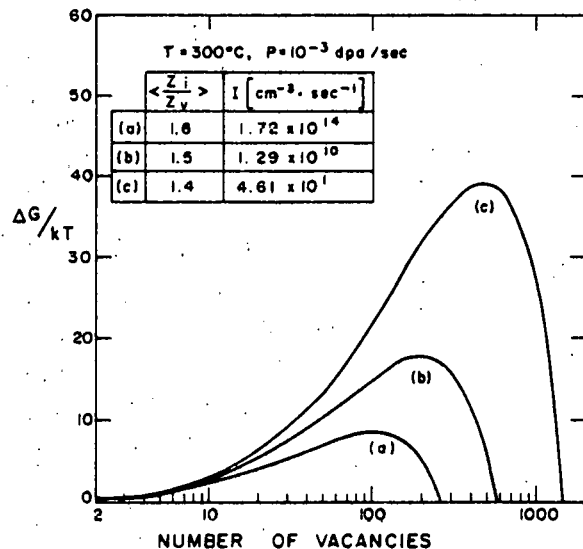


Figure 2 Ratio of the capture efficiencies for (above) interstitials, Z_i , and vacancies, Z_v , as a function of the loop radius.

Figure 3 Nucleation barrier for vacancy-type (right) loops. Dose rate is typical for ion-bombardment experiments.

temperatures of 200 and 400°C, the recombination volumes are 34 Ω and 27 Ω , respectively. It was further assumed that 10% of all displacement events contribute to freely migrating point defects.

Using the above parameters as well as those of Ref. 12, $\Delta G(R)$ can be computed. Typical results are shown in Fig. 3 for the nucleation barrier of vacancy-type loops. The inserted table gives also the steady-state nucleation rates. It is seen that the nucleation barrier increases with decreasing average capture ratio $\langle Z_i/Z_v \rangle$ with a concomitant sharp drop in the nucleation rate. This is most dramatically demonstrated by the results of Figure 4 which shows that vacancy-type loops can only nucleate in a material whose sinks are highly biased for preferential interstitial absorption. This condition is only met when small dislocation loops constitute the dominant sink. As no nucleation barrier exists for interstitial-type loops (4), they can readily and abundantly form. Therefore, they produce a highly biased sink structure which favors also the nucleation of vacancy-type loops. However, as the loops grow to larger sizes, the average capture ratio $\langle Z_i/Z_v \rangle$ drops continuously until it approaches a value of 1.2 typical of a dislocation network. It is this decrease of $\langle Z_i/Z_v \rangle$ which eventually terminates the nucleation of vacancy-type loops, rather than the increase of the sink density. To demonstrate this more clearly, Table 1 gives the steady-state nucleation rates for two sink densities. Clearly, the sink density has a negligible effect on the nucleation rate of vacancy-type loops.



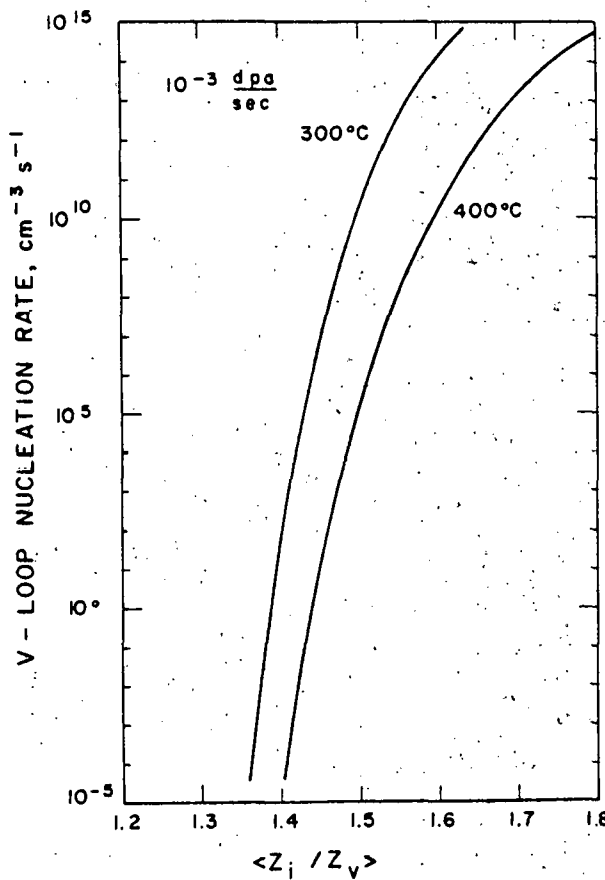


Figure 4 Nucleation rate for vacancy-type loops as a function of the average capture ratio.

A further condition for the nucleation of vacancy-type loops is that the re-emission rate of vacancies from the loops be small in comparison with the capture rate of vacancies. Consequently, their nucleation is only possible at low temperatures. The temperature limit depends, however, on the Frenkel pair production rate, as can be clearly seen from the results in Fig. 5. For ion bombardment conditions with a typical production rate of 10^{-3} dpa/s, the upper temperature limit is about 420°C. In contrast, for breeder reactor irradiations with 10^{-6} dpa/s, the temperature limit is at about 320°C.

Discussion

The conditions for the nucleation of vacancy-type loops are that their interstitial capture efficiency be lower than that of interstitial-type loops; that the temperature of irradiation be lower than a critical value which depends on the dose rate; and that the average interstitial capture efficiency for the total sink structure be larger than about 1.45. In order to satisfy the last condition, the sink structure must be dominated by small dislocation loops.

Since there exists no significant barrier for interstitial loop nucleation (4) they form immediately after the irradiation begins. In fact, calculations by Hayns (15) and by Ghoniem and Cho (16) have shown that interstitial loop densities of the order of 10^4 loops/cm³ are reached within less than a second during fast reactor irradiation in materials with an initial line dislocation density of 10^8 cm⁻². For this value of the loop density, the average radius need only be of the order of 3 bo to obtain a loop sink strength equal to the dislocation sink strength. In this case, the

TABLE 1. Effect of Sink Density on Vacancy-Type Loop Nucleation ($\text{cm}^{-3} \text{s}^{-1}$) at $T = 400^\circ\text{C}$ and for 10^{-3} dpa/s

Average Capture Ratio	Sink Density, cm/cm^2	
	5×10^8	10^{10}
1.4	4.36×10^{-5}	4.23×10^{-5}
1.5	1.65×10^5	1.59×10^5
1.6	1.52×10^{10}	1.48×10^{10}

interstitial capture averaged over all sinks is large, and vacancy-loop nucleation can proceed. If the initial line dislocation density is 10^9 cm⁻², the interstitial loop density reaches a lower value (15,16) around 10^{13} loops/cm³. In order for the loops to become a sink of comparable strength, they must now grow to a radius of about 30 bo. As seen from Fig. 2, however, their capture efficiency is about 1.3 at that radius. The average interstitial capture efficiency is then 1.25, which is too low for vacancy-type loop nucleation to occur. Therefore, we estimate that the initial dislocation line density can be no higher than 5×10^8 cm⁻² for vacancy-type loops to form.

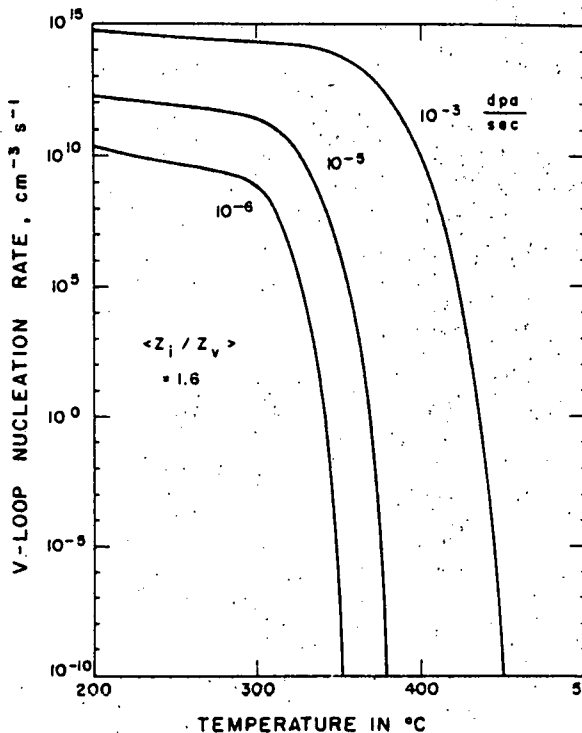


Figure 5 Nucleation rate for vacancy-type loops as a function of temperature and dose rate.

The nucleation rates given above are for the steady-state which is reached after the incubation time. For a dose rate of 10^{-6} dpa/s and an irradiation temperature of 300°C , the incubation time for vacancy-type loop nucleation was found to be about 12 hours, and it decreases with increasing temperature and increasing dose rate. This incubation time is much longer than for the interstitial-type loop formation, but in general very short compared to the total irradiation time.

A well documented case of the simultaneous formation of both loop types is the one for zirconium alloys (17). Here, both loop types form on the prism planes but not on the basal planes. The observed loop densities are between 10^{16} and 5×10^{16} cm^{-3} . The dislocation density, even in cold-worked materials, is 10^8 cm^{-2} or lower. Therefore, the conditions for vacancy loop nucleation are certainly met. Considering these loop densities and the observed (17) loop diameters (30 to 90 nm), the ratio of the loop radius to the loop separation distance is only of the order of 0.1. Therefore, we conclude that proximity effects on the capture efficiencies are indeed small and of secondary importance compared to the effect produced by nonlinear elasticity.

Acknowledgements

This research was supported by the Division of Basic Energy Sciences, U.S. Department of Energy, under contract ER-78-S-02-4861 with the University of Wisconsin.

References

1. W.G. Wolfer and M. Ashkin, *J. Appl. Phys.* **46**, 547; **46**, 4108 (1975).
2. W.G. Wolfer and A. Si-Ahmed, *Phys. Letters* **76A**, 341 (1980).
3. R. Bullough, M.R. Hayns, and C.H. Woo, Harwell Report TP.783, Feb. 1979.
4. F.A. Garner, W.G. Wolfer, and H.R. Brager, in *Effects of Radiation on Structural Materials*, 9th Internat. Symp., ASTM STP 683, 1979, p. 160.
5. A. Seeger and U. Goesele, *Phys. Letters* **61A**, 423 (1977).
6. W.G. Wolfer and M. Ashkin, *J. Appl. Phys.* **47**, 791 (1976).
7. A. Seeger and P. Haasen, *Phil. Mag.* **3**, 470 (1958).
8. M.W. Guinan and D.J. Steinberg, *J. Phys. Chem. Solids* **35**, 1501 (1974).
9. P. Ehrhart, *J. Nucl. Materials* **69** & **70**, 200 (1978).
10. J.L. Katz and H. Wiedersich, *J. Chem. Phys.* **55**, 1414 (1971).
11. K.C. Russell, *Acta Met.* **19**, 753 (1971).
12. W.G. Wolfer and M.H. Yoo, in *Rad. Effects and Tritium Technology for Fusion Reactors*, Proc. of the Internat. Conf., Eds. J.S. Watson, F.W. Wiffen, CONF-750989, 1976, Vol. II, p. 458.
13. W.G. Wolfer and A. Si-Ahmed, to be published.
14. M. Nakagawa, K. Boening, P. Rosner, and G. Vogel, *Phys. Rev. B* **16**, 5285 (1977).
15. M.R. Hayns, *J. Nucl. Materials* **56**, 267 (1975).
16. N.M. Ghoniem and D.D. Cho, *Phys. Stat. Sol.* (a) **54**, 171 (1979).
17. D.O. Northwood, R.W. Gilbert, L.E. Bahen, P.M. Kelly, R.G. Blake, A. Jostens, P.K. Madden, D. Faulkner, W. Bell, and R.B. Adamson, *J. Nucl. Materials* **79**, 379 (1979).